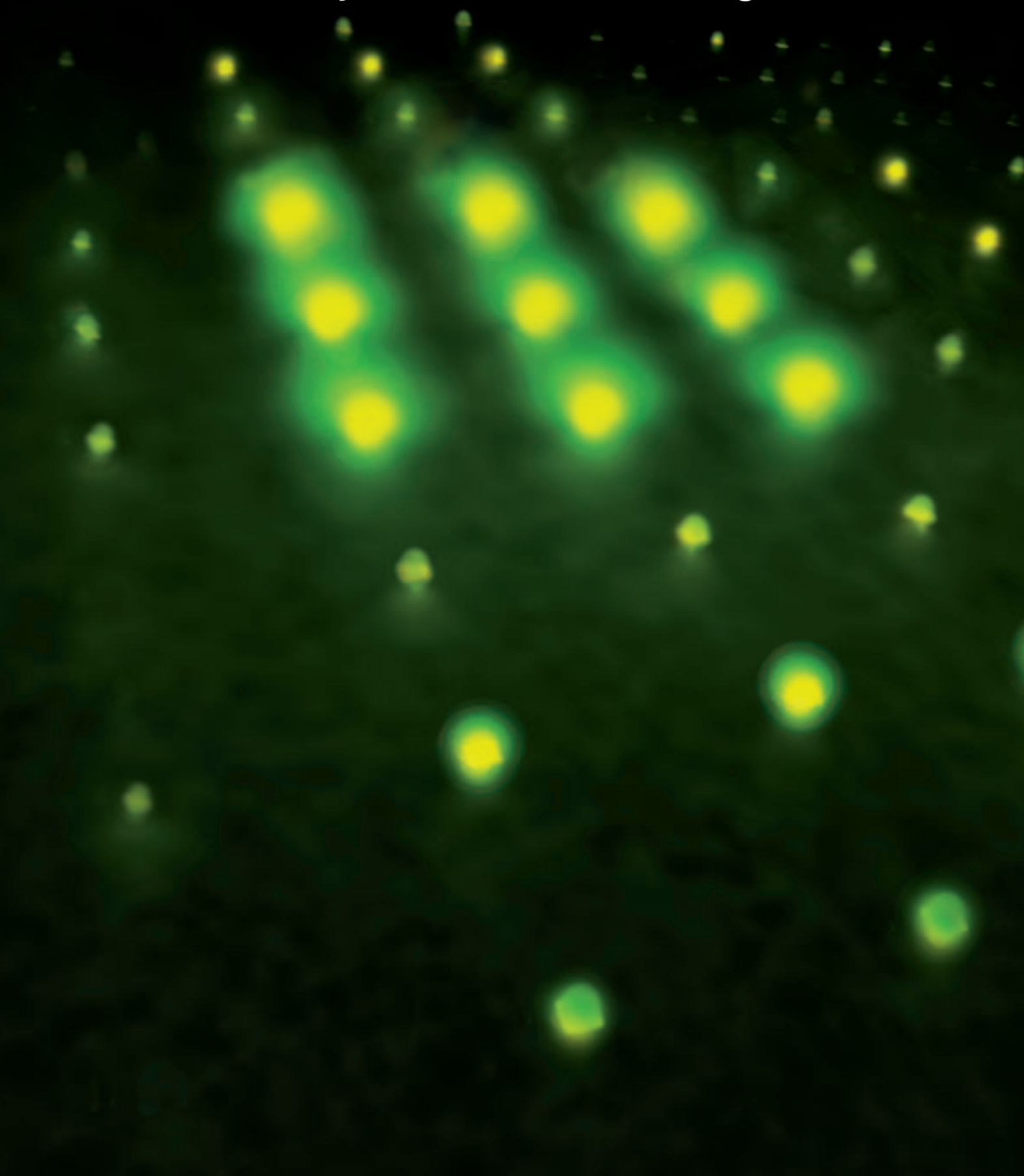# Extraordinary IR Transmission with Metallic Arrays of Subwavelength Holes

**Subwavelength holes and disappearing diffraction spots have implications for sensors and enhanced surface spectroscopy.**

What happens to the optical properties of metal films with periodic arrays of holes when the width of the holes becomes smaller than the wavelength of the probing light? Under certain coupling circumstances (such as with prisms, gratings, waveguides, or surface roughness), light can be used to excite coherent oscillations in the metal's conducting electrons at a dielectric/metal interface; that is, surface plasmons (SPs) can be excited (*1*). SPs are routinely used in analytical applications of attenuated total reflection (ATR; *2*, *3*); waveguide-coupled plasmon resonance experiments (*4*, *5*); and surface-enhanced Raman spectroscopy (*6*) to detect minute changes in interface properties. But can simple metallic microarrays also excite SPs? When the holes and periodicity are larger than the wavelength of the probing light, we expect to see the transmission of a diffraction pattern. What happens to the diffraction pattern when the wavelength becomes larger than the width of the holes? What happens to the light that was transmitted in diffraction spots? We know that individual metallic waveguides have nominal wavelength cutoffs at twice the hole width (*7*); can any light be transmitted by periodic arrays at wavelengths longer than the cutoff?

In this article, we will address these questions and show circumstances that lead to unusually large transmissions. The basics of this type of SP-mediated transmission will be briefly described; we will explain how these properties are moved into the IR region and applied to obtain enhanced IR absorption spectroscopy of surface molecules. Finally, we will discuss stacks of mesh and the potential for sensors.

## Overview

Periodic metal nanoarrays of subwavelength apertures were first shown by Ebbesen and co-workers to transmit more visible light than is incident upon the apertures; that is, light initially incident upon optically thick metal is still transmitted without scattering from the incident beam (*8*, *9*). Because a full review of this work would be a massive undertaking, let it suffice that Ebbesen's 1998 *Nature* paper (*8*) has been cited 561 times at the writing of this article.

The extraordinary transmission effect is generally described as an SP-mediated mechanism (*9–12*). The periodicity of the mesh couples with the incident light to produce an SP type of polariton, which is an oscillation of the metal's conducting electrons at the surface of the metal (*1*). The SPs

**James V. Coe • Shaun M. Williams • Kenneth R. Rodriguez •**

**Shannon Teeters-Kennedy • Alexandra Sudnitsyn • Frank Hrovat**
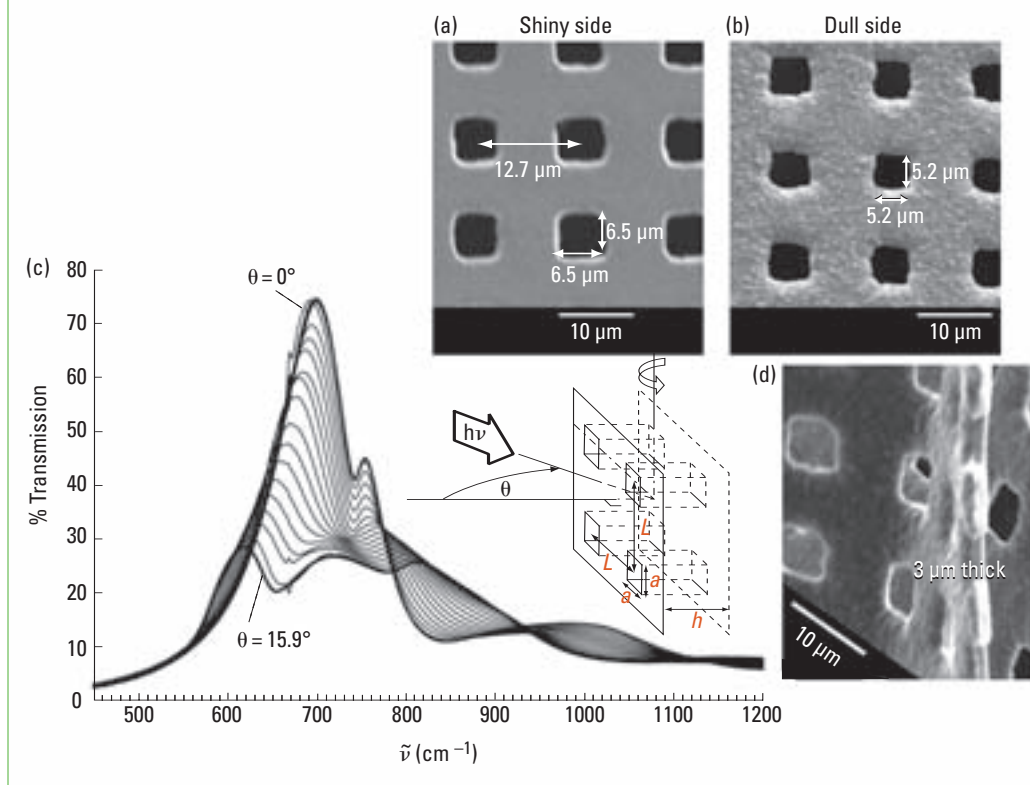
**OHIO STATE UNIVERSITY**

**FIGURE 1.** (a, b, d) Scanning electron microscopy images of the nickel mesh, characterizing the structure of the arrays and revealing an open area of ~17%. (c) The zero-order FTIR transmission spectra and the mesh's geometry are shown as the mesh is rotated up to 15.9° from perpendicular incidence.

propagate along the surface of the mesh, perhaps on both sides, to another hole where they decouple, producing photons that emerge in the same direction as the incident beam. Studies of ultrafast behavior, entangled photons, polarization effects, and SP propagation between separated subwavelength arrays have indicated that, fundamentally, the phenomena are single-photon processes that can preserve phase and polarization, at least under some conditions (*13–17*).

The positions of resonances in the transmission spectra are governed by the hole-to-hole spacing in the periodic array. Standard FTIR spectrometers cover the region of fundamental molecular vibrations of ~400–4400 $cm^{-1}$, corresponding to wavelengths of 25–2.3 μm, so a hole-to-hole spacing of ~13 μm works well. Moller et al. used grids that had apertures of various shapes to first demonstrate enhanced IR transmissions (*18*). To move Ebbesen's extraordinary transmission effect into the IR (*19*), we used the finest commercially available metal mesh (Precision Eforming). It comes in 15 × 15 cm sheets and is currently only available in nickel. The mesh holes are arranged as a square lattice with a hole-to-hole spacing *L* of 12.7 μm and a thickness *h* of ~3 μm. The holes are primarily square in cross section, though the corners are rounded. The holes have a width *a* of ~6.5 μm on the smooth side of the mesh, which tapers to a minimum of ~5.2 μm on the rougher side (Figures 1a and 1b).

Unpolarized, zero-order, IR transmission spectra of the mesh and its geometry are shown in Figure 1c. These spectra were

recorded at a resolution of 4 $cm^{-1}$ with normalization for the changing cross section of the aperture as the mesh is rotated. In spite of the mesh having an open area of ~17%, we observed transmission of 75% at 700 $cm^{-1}$ at perpendicular incidence (θ = 0°), which corresponds to an enhancement of 4.4 over the fractional open area. This enhancement clearly shows that transmission is dominated by light that initially strikes optically thick metal; that is, the mesh exhibits Ebbesen's extraordinary transmission effect.

## SPs, dispersion, and diffraction

The transmission resonances change their positions in the spectra as the mesh is rotated relative to the incoming beam of the spectrometer. Such measurements can be used to characterize the dispersion of these features. Different optical phenomena show different dispersion trends, so such studies are important in assessing the role of SPs. The primary resonance breaks into 3 branches (Figure 1c) as θ goes from 0 to 15.9°. More detailed studies indicate that the first branch (615 $cm^{-1}$ at θ = 15.9°) and the third branch (815 $cm^{-1}$ at θ = 15.9°) are p-polarized features that disperse with trends similar to those of SPs on smooth air/metal interfaces (*15*). The second branch (715 $cm^{-1}$ at θ = 15.9°) is broader than the other two branches, is an s-polarized feature, and disperses with a very flat trend (*15*). The details of these dispersion studies are currently a challenging problem of great interest in optical physics, and theorists are still grappling with the details.

A connection also exists to well-known diffraction properties. Photographs of diffraction patterns produced by three different visible lasers on the nickel mesh with the same geometry are shown in Figures 2a–2c. Each different laser produces similar grid patterns with an oscillating pattern of spot intensities that generally diminishes as one moves away from the origin. Spots are no longer transmitted at some distance from the center (beyond the edges of these images), beyond what is known as the Airy disk. The same labels for diffraction spots, that is, integer steps from the origin along the reciprocal lattice *i*, *j* (as given in the red diffraction image in Figure 2c), are also used to label the transmission resonances. To understand this, imagine how these patterns change as we move into the IR region. As the visible wavelength

gets larger from left to right, a larger spacing between adjacent diffraction spots is evident. Consequently, fewer diffraction spots appear within the Airy disk. This trend continues as we move to the longer wavelengths of the IR region. The observed transmission resonances occur at wavelengths for which diffraction spots are outside the Airy disk and are no longer transmitted. Instead, they are trapped on the mesh as evanescent waves that may launch SPs (*20*).

A zero-order IR transmission spectrum of a nickel mesh with these same lattice constants but with holes closed down to ~3 μm is shown in Figure 2d (*21*). The resonances are labeled by the diffraction spots *i,j* that are no longer transmitted and are trapped on the surface of the mesh. The evanescent waves can
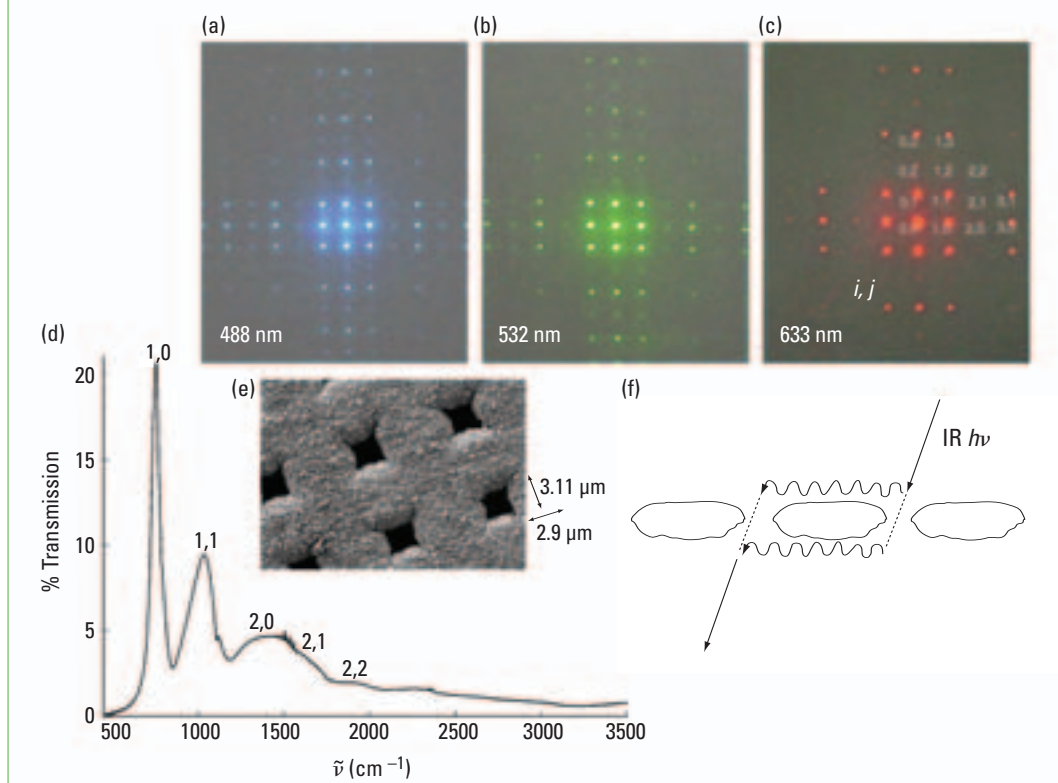


**FIGURE 2.** (a–c) Photographs of transmitted diffraction patterns produced by three different visible lasers on the nickel mesh with the same geometry. (d) A zero-order IR transmission spectrum of a nickel mesh with the same lattice constants as in Figure 1 but with (e) ~3-μm holes. (f) Schematic of how light travels through the mesh.

launch SPs (if the metal can support them) that mediate transmission through the holes without scattering from the incident beam. Hole size has a dramatic effect on the appearance of transmission spectra, and the smaller hole size reveals more resonances than the mesh of Figure 1 (*22, 23*). An approximate equation for the spectral position of transmission resonances is

$$\widetilde{\nu}_{\max} = \frac{\sqrt{(i^2 + j^2)}}{L n'_{\text{eff}}}$$

in which the pairs *i,j* are the integer steps from the origin along the reciprocal lattice and $n'_{\text{eff}}$ is the effective index of refraction. This last parameter varies in practice from 1 to ~1.1. Analytical expressions for $n'_{\text{eff}}$ are known for the case of a smooth air/metal interface, but the case of periodic mesh arrays is still a topic of theoretical investigation.

Nickel is not generally thought of as a good metal for SP work (*19*). Metals can support SPs because of their complex dielectric function, which can be written as $\varepsilon_{\text{m}} = \varepsilon'_{\text{m}} + i\varepsilon''_{\text{m}}$. SPs can be supported on a semi-infinite, smooth air/metal interface if $|\varepsilon'_{\text{m}}| > \varepsilon''_{\text{m}}$ (*1*). This condition is true for silver, gold, and copper at wavelengths >260, 500, and 338 nm, respectively; therefore, these are the metals of choice for SP work in the visible region (*24*). This condition becomes true for nickel at 2496 nm, or 4006 cm$^{-1}$, so nickel will support SPs in the mid-IR region. At 3000 cm$^{-1}$, the Lorentz–Drude model value (*24*) of nickel's dielectric function is −134 + $i$100, and at 700 cm$^{-1}$, the value is −2361 + $i$1466,

which are both very different from those of the noble metals in the visible. When the incident light is pushed into the IR, other metals (such as tungsten, platinum, palladium, and chromium) will also support SPs.

Two observations from enhanced IR absorption studies of self-assembled monolayers (SAMs) pertain to a simple picture of the extraordinary transmission phenomenon. Absorption spectra of nanocoated mesh can be recorded at different angles relative to the spectrometer's beam (just as in the dispersion studies mentioned previously); this moves the resonances relative to fixed vibration absorption bands (*25*). So far, no enhancements have been observed when a transmission resonance lies directly upon a vibration band; that is, the same absorption spectrum is observed regardless of the angle of the mesh to the spectrometer beam. This suggests that the SPs are not bouncing back and forth within the hole as with an etalon (*26*); rather, absorption is due primarily to propagation along the front and back metal surfaces. Upon taking the ratio of our absorptions to those of single-pass reflection absorption IR spectroscopy (RAIRS) experiments (with well-characterized path lengths), we obtain effective path lengths comparable with or smaller than *L*. This suggests that the extraordinary transmission process is dominated by propagation on the front or back surface of an adjacent hole (Figure 2f schematic). Because SPs can travel considerably farther than *L* on smooth, unperforated metal surfaces, this is an important conclusion.
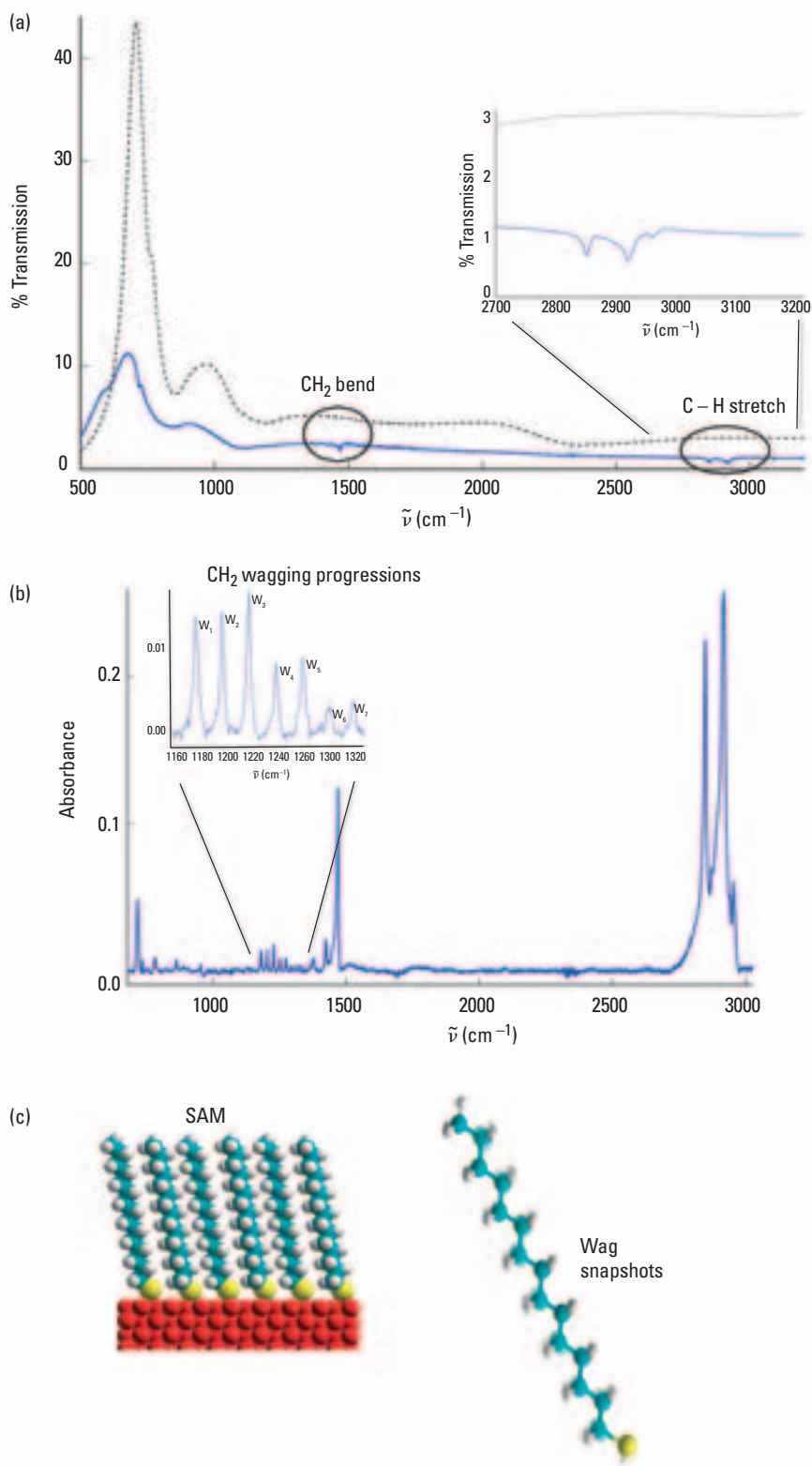
**FIGURE 3.** (a) Transmission spectra of copper-coated nickel mesh before (dotted trace) and after (solid trace) it is coated with a 14-carbon-long alkanethiol SAM. Molecular absorptions (circled and expanded areas) are apparent even before conversion to (b) the corresponding absorption spectrum. (c) A tetradecanethiol SAM on copper and the extremes of $CH_2$ wagging vibrations. The expanded absorption spectrum in (b) shows progressions of the wagging vibrations that are only evident for all-trans configurations of the hydrocarbon chains.

## Enhanced IR absorption spectroscopy

The extraordinary IR transmission of these meshes means that we can use them to obtain enhanced IR absorption spectra of molecular species at the metal's surface simply by placing the mesh in the sample position of a standard FTIR spectrometer in transmission mode. Figure 3a shows transmission spectra recorded at perpendicular incidence of copper-coated nickel mesh before and after the application of a tetradecanethiol SAM (27). The resonances shift in position and are damped in intensity after the application of a nanocoating; this shift is the wavelength-scanned equivalent of ATR studies.

More importantly, however, dips in the transmission are due to molecular absorptions (Figure 3a, circled and expanded areas) that are evident even before conversion to absorption spectra. This is impressive because the nanocoating is only one molecule (~2 nm) thick. The very enhanced absorptions are accompanied by very ill behaved backgrounds due to the transmission resonances. Points are chosen systematically along the transmission trace, excluding the molecular absorption features, and the points are fitted with a spline function to obtain a smooth background.

The corresponding absorption spectrum [−log(transmission/spline-smoothed background)] is presented in Figure 3b. Absorptions in the CH stretch region are >100-fold enhanced over those reported in RAIRS studies (28–30). The region of Snyder's $CH_2$ wagging progression (31) in the absorption spectrum can be seen in the expansion. These vibration progressions are only observable for ordered, all-trans configurations of the hydrocarbon chains. In general, these spectra are characteristic of the phase, orientation, and binding of the molecules in nanocoatings. A tetradecanethiol SAM and a snapshot at the extremes of the normal motions for one of the $CH_2$ wagging progression vibrations are shown in Figure 3c.

It is also possible to use the extraordinary IR transmission of these metallic meshes to record IR absorption spectra of intermediates and products of reactions on catalytic metal surfaces. We have examined the well-known industrial pro-

cess of the transformation of methanol on copper oxide to formaldehyde (*25*). Pieces of nickel mesh were electrochemically coated with copper to reduce the hole size to ~4 µm and exposed to moist air for several weeks to oxidize the surface. This process significantly diminished the transmission resonances. Next, the mesh was exposed to a drop of water, which took ~10 min to evaporate as monitored by IR transmission scans. Then, a drop of methanol was added, and IR transmission scans were recorded in time, one after another, as quickly as possible. Spectra were recorded under conditions whereby the adsorbed methoxy radical intermediate could be detected before it was converted to formaldehyde.

The catalytic process on the molecular scale and the IR absorption spectra as a function of time are shown in Figures



**FIGURE 4.** (a) Molecular-scale schematic of the catalytic transformation of methanol to formaldehyde on copper oxide. (b) IR absorption spectra vs time after a drop of methanol is added to an oxidized, copper-coated nickel mesh that had been activated with a drop of water. (c) The spectrum of $CH_2O(ads)$ recorded over the course of 1 h.

4a and 4b. These spectra are offset, with the first at the top and the last, 2 h later, at the bottom. The first few spectra are separated by ~20-s intervals and show a prominent methoxy radical band (1029 cm$^{-1}$), which goes away in ~45 s as the spectrum of adsorbed formaldehyde rises and persists for ~2 h. The spectrum of $CH_2O(ads)$ is isolated at various times over 1 h (Figure 4c). Metallic surfaces give rise to image charges of molecules, which cancel the dipole derivatives of vibrations parallel to the surface (*32*) but enhance the intensity of vibrations perpendicular to the surface. This effect is clearly evident in the intensities of the observed vibration bands.

## Mesh stacks and future work

We have reported several preliminary studies showing that if two meshes are stretched and stacked, one upon the other, then they still exhibit Ebbesen's extraordinary transmission effect (*19, 21*). A 4-mesh stack was made that still transmitted 22% of the incident FTIR beam (*21*). In fact, we now know that if two meshes are stacked in registry (with aligned lattice axes, but offset so that the holes of the first mesh are followed by metal with the second mesh) so that no openings occur directly through the stack, the system still can transmit 5–10% of the incident IR beam to the spectrometer's detector! Detailed dispersion and polarization studies of doubled stacks will be reported shortly. A schematic of a double-stack mesh, each mesh with its own nanocoating, and various ways that IR photons might travel through the system are shown in Figure 5a. Such systems
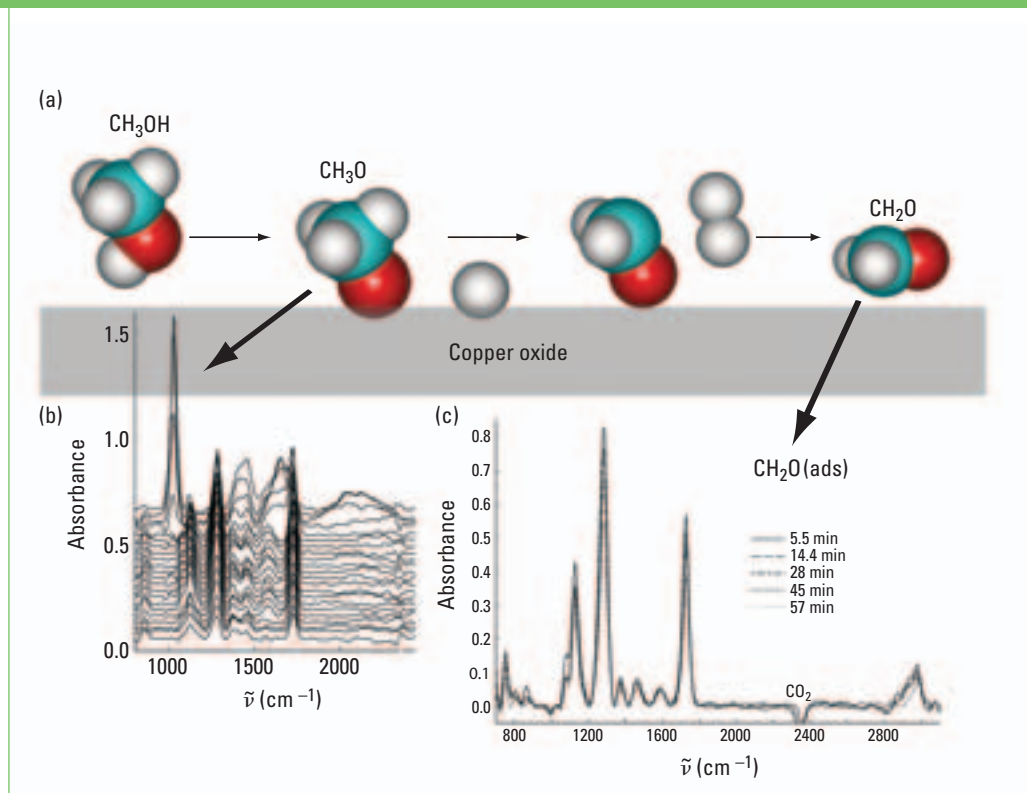
achieve extensive interactions of the IR beam with the surface, and it is likely that SPs travel between the two layers of metal. We have reported nonlinear gains in absorption with alkanethiol coatings of a two-mesh stacked system (*19, 21*).

The stacked arrangement is of particular interest because one can imagine situations in which the two pieces of metal can be insulated from each other and can be used as electrodes for a capacitive assay of the molecules trapped between the two pieces of mesh. The combination of optical and IR absorption with an electrical assay based on this arrangement could create a powerful sensor. Future work will focus on insulating the two pieces of mesh via self-assembled alkanethiol monolayers as well as additional phospholipid bilayers (*21*). Figure 5b is an expansion of the circled region in Figure 5a. We have produced phospholipid bilayers on top of alkanethiol SAMs (*21*); these bilayers constitute half of the stacked assembly (Figure 5b, far right). It would be interesting to see whether the same forces at work in the construction of phospholipid bilayers in cell membranes could be used to self-assemble multilayered nanoassemblies between the two mesh electrodes over a macroscopic area. If this could be accomplished, then there would be one cell-like model membrane in the center of the construction.

We have imagined exposing the perforated mesh to a defined vapor pressure of water, which would be adsorbed at the polar headgroup regions of the phospholipid bilayers; this would essentially solvate the central cell-membrane model bilayer (Figure 5b, middle). Then, we could add membrane-bound proteins as
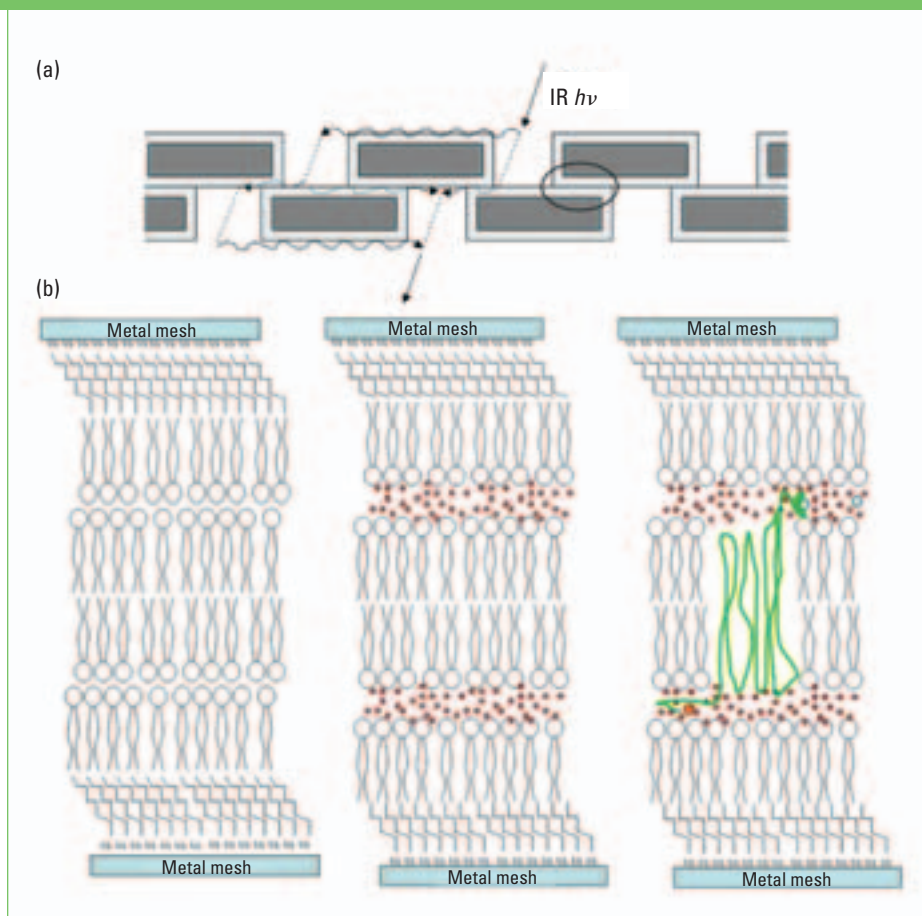
**FIGURE 5.** (a) A nanocoated two-mesh stack that transmits IR light even though there is no path straight through the material. The circled region is expanded (b) to reveal a nanoassembly produced by using phospholipid bilayers on top of alkanethiol SAMs.

the system was constructed, effectively isolating them (Figure 5b, far right). The extraordinary IR transmission of metallic meshes offers the potential for an exciting new class of sensors with an unprecedented direct IR absorption assay of the molecular details of nanoassemblies.

*James V. Coe is an associate professor; Shaun M. Williams, Kenneth R. Rodriguez, and Shannon Teeters-Kennedy are graduate research associates; and Alexandra Sudnitsyn and Frank Hrovat are undergraduate researchers at Ohio State University. Coe's research interests include connecting the properties of small atoms, molecules, and clusters to the bulk and special properties of systems in the nanosize regime. Williams is interested in the physics of SPs. Rodriguez's research focuses on IR study of alkanethiol SAMs, catalytic reactions of alcohols on nickel and copper, and single-walled carbon nanotubes. Teeters-Kennedy's research focuses on IR studies of cell membranes, enhanced absorption of molecular systems on mesh, and SP dispersion in multi-stacked systems. Sudnitsyn is interested in cells in microchannels. Address correspondence about this article to Coe at Ohio State University, Department of Chemistry, 100 W. 18th Ave., Columbus, OH 43210-1173 (coe1@osu.edu).*

## References

(1)  Raether, H. *Surface Plasmons on Smooth and Rough Surfaces and on Gratings*; Springer-Verlag: Berlin; 1988.

(2)  Kretschmann, E.; Raether, H. Z. *Naturforsch., A: Phys. Sci.* **1968**, *23*, 2135–2136.

(3)  Otto, A. Z. *Phys. A* **1968**, *216*, 398–410.

(4)  Salamon, Z.; Macleod, H. A.; Tollin, G. *Biophys. J.* **1997**, *73*, 2791–2797.

(5)  Salamon, Z.; et al. *Biochim. Biophys. Acta* **1994**, *1195*, 267–275.

(6)  Nie, S.; Emory, S. R. *Science* **1997**, *275*, 1102–1106.

(7)  Jackson, J. D. *Classical Electrodynamics*, 3rd ed.; Wiley: New York, 1999.

(8)  Ebbesen, T. W.; et al. *Nature* **1998**, *391*, 667–669.

(9)  Ghaemi, H. F.; et al. *Phys. Rev. B.* **1998**, *58*, 6779–6782.

(10) Thio, T.; et al. *J. Opt. Soc. Am. B* **1999**, *16*, 1743–1748.

(11) Thio, T.; et al. In *Integrated Photonics Research*; Trends in Optics and Photonics, Vol. 58; Optical Society of America: Princeton, NJ, 2001, IMB3/1–IMB3/3 (accession no. 2001: 838261).

(12) Barnes, W. L.; Dereux, A.; Ebbesen, T. W. *Nature* **2003**, *424*, 824–830.

(13) Dogariu, A.; et al. *Opt. Lett.* **2001**, *26*, 450–452.

(14) Altewischer, E.; van Exter, M. P.; Woerdman, J. P. *Nature* **2002**, *418*, 304–306.

(15) Barnes, W. L.; et al. *Phys. Rev. Lett.* **2004**, *92*, 107,401–107,405.

(16) Devaux, E.; et al. *Appl. Phys. Lett.* **2003**, *83*, 4936–4938.

(17) Altewischer, E.; et al. *Opt. Lett.* **2005**, *30*, 90–92.

(18) Moller, K. D.; et al. *Infrared Phys. Technol.* **1999**, *40*, 475–485.

(19) Williams, S. M.; et al. *J. Phys. Chem. B* **2003**, *107*, 11,871–11,879.

(20) Vigoureux, J. M. *Opt. Commun.* **2001**, *198*, 257–263.

(21) Williams, S. M.; et al. *Nanotechnology* **2004**, *15*, S495–S503.

(22) Williams, S. M.; et al. *Appl. Phys. Lett.* **2004**, *85*, 1472–1474.

(23) Degiron, A.; et al. *Appl. Phys. Lett.* **2002**, *81*, 4327–4329.

(24) Rakic, A. D.; et al. *Appl. Opt.* **1998**, *37*, 5271–5283.

(25) Williams, S. M.; et al. *J. Phys. Chem. B* **2004**, *108*, 11,833–11,837.

(26) Martin-Moreno, L.; et al. *Phys. Rev. Lett.* **2001**, *86*, 1114–1117.

(27) Rodriguez, K. R.; et al. *J. Chem. Phys.* **2004**, *121*, 8671–8675.

(28) Laibinis, P. E.; et al. *J. Am. Chem. Soc.* **1991**, *113*, 7152–7167.

(29) Jennings, G. K.; et al. *Langmuir* **1998**, *14*, 6130–6139.

(30) Ron, H.; et al. *J. Phys. Chem. B* **1998**, *102*, 9861–9869.

(31) Snyder, R. *J. Mol. Spectrosc.* **1960**, *4*, 411–434.

(32) Camplin, J. P.; McCash, E. M. *Surf. Sci.* **1996**, *360*, 229–241.